

**INSTITUTO TECNOLÓGICO DE AERONÁUTICA**



**Pedro Kuntz Puglia**

**OPTIMAL IMPULSIVE ORBITAL MANEUVER  
SYNTHESIS THROUGH DIRECT OPTIMIZATION**

Final Paper  
2025

**Course of Aerospace Engineering**

**Pedro Kuntz Puglia**

**OPTIMAL IMPULSIVE ORBITAL MANEUVER  
SYNTHESIS THROUGH DIRECT OPTIMIZATION**

Advisor

Prof. Dr. Willer Gomes dos Santos (ITA)

Co-advisor

Prof. Emilien Flayac (ISAE-SUPAERO)

**AEROSPACE ENGINEERING**

SÃO JOSÉ DOS CAMPOS  
INSTITUTO TECNOLÓGICO DE AERONÁUTICA

2025

**Cataloging-in Publication Data**  
**Documentation and Information Division**

Puglia, Pedro Kuntz  
Optimal Impulsive Orbital Maneuver Synthesis through Direct Optimization / Pedro Kuntz  
Puglia.  
São José dos Campos, 2025.  
46f.

Final paper (Undergraduation study) – Course of Aerospace Engineering– Instituto Tecnológico de Aeronáutica, 2025. Advisor: Prof. Dr. Willer Gomes dos Santos. Co-advisor: Prof. Emilien Flayac.

1. Optimization. 2. Control. 3. Orbital Mechanics. I. Instituto Tecnológico de Aeronáutica.  
II. Title.

**BIBLIOGRAPHIC REFERENCE**

PUGLIA, Pedro Kuntz. **Optimal Impulsive Orbital Maneuver Synthesis through Direct Optimization**. 2025. 46f. Final paper (Undergraduation study) – Instituto Tecnológico de Aeronáutica, São José dos Campos.

**CESSION OF RIGHTS**

AUTHOR'S NAME: Pedro Kuntz Puglia

PUBLICATION TITLE: Optimal Impulsive Orbital Maneuver Synthesis through Direct Optimization.

PUBLICATION KIND/YEAR: Final paper (Undergraduation study) / 2025

It is granted to Instituto Tecnológico de Aeronáutica permission to reproduce copies of this final paper and to only loan or to sell copies for academic and scientific purposes. The author reserves other publication rights and no part of this final paper can be reproduced without the authorization of the author.

---

Pedro Kuntz Puglia  
Rua H8C, Ap. 303  
12.228- 462 – São José dos Campos- SP

# OPTIMAL IMPULSIVE ORBITAL MANEUVER SYNTHESIS THROUGH DIRECT OPTIMIZATION

This publication was accepted like Final Work of Undergraduation Study

---

Pedro Kuntz Puglia

Author

---

Willer Gomes dos Santos (ITA)

Advisor

---

Emilien Flayac (ISAE-SUPAERO)

Co-advisor

---

Profa. Dra. Cristiane Martins

Course Coordinator of Aerospace Engineering

São José dos Campos: junho ??, 2025.

# Abstract

This work presents the implementation of an orbital maneuver solver under two-body Keplerian dynamics and impulsive thrust model. The control task consists of finding the trajectory between two given states, in a fixed amount of time, minimizing fuel consumption. Optimal control formalism, in the form of the control Hamiltonian, is applied to the problem to uncover the consacrated primer vector theory, which can inform hyperparameter choice. A Julia interface to the recognized Ipopt solver is used to implement a relaxation method for the optimizer. A Lambert problem solver is used to supply a feasible initial guess to the solver. Finally, the results of direct optimization and primer vector theory are compared to the established Hohmann transfer analytical results to validate the implementation.

# Contents

<b>1</b>	<b>Introduction . . . . .</b>	<b>7</b>
1.1	Problem statement . . . . .	9
1.2	Hypotheses . . . . .	9
1.3	Objectives . . . . .	10
1.4	Justification . . . . .	11
1.5	Work structure . . . . .	11
<b>2</b>	<b>Theory and fundamentals . . . . .</b>	<b>12</b>
2.1	Optimal Control . . . . .	12
2.2	Orbital Mechanics . . . . .	15
2.2.1	Two Body Motion . . . . .	15
2.2.2	Orbital Perturbations . . . . .	17
2.2.3	Lambert's Problem . . . . .	18
2.2.4	Variational State Transition Matrix . . . . .	19
2.3	Orbital Maneuvers . . . . .	19
2.3.1	Constant specific impulse model . . . . .	20
2.3.2	Impulsive propulsion model . . . . .	21
2.4	Primer vector theory . . . . .	24
2.4.1	Conservative Orbital model . . . . .	24
<b>3</b>	<b>Bibliographic review . . . . .</b>	<b>28</b>
3.1	Lambert Problem . . . . .	28
3.2	Primer Vector theory . . . . .	29
3.3	Direct Optimization . . . . .	29

---

<b>4</b>	<b>Methodology</b>	31
4.1	Orbit Propagation	31
4.2	Optimization algorithm with fixed number of impulses	32
4.3	Primer vector algorithm	32
4.4	Nonlinear solver	32
4.5	Lambert problem implementation	33
4.6	Optimal impulsive maneuver problem statement	35
<b>5</b>	<b>Results</b>	37
5.1	Two Body	37
5.1.1	Circle to Circle	37
5.1.2	Noncoplanar rendez-vous	37
5.2	J2 Perturbed	39
5.2.1	Circle to Circle	39
5.2.2	Noncoplanar rendez-vous	39
5.3	J2 and Drag	41
5.3.1	Circle to Circle	41
<b>6</b>	<b>Planning</b>	43
	BIBLIOGRAPHY	44

# 1 Introduction

Space exploration relies on clever resource management, since satellites have a finite amount of resources (propellant and other consumables) to fulfill their mission. Up to this date, all space hardware is expendable, that is, when the consumables required for mission maintenance are finished, the mission ends, marking the end of the exploration of a very expensive engineered system. Thus the need for optimization arises in this domain.

Contrary to science fiction, where spaceships seem to be constantly propelled by their thrusters, real life satellites change their courses in discrete moments of maximum thrust application, surrounded by (usually long) coasting periods. This is due to the relatively high power delivered by traditional rocket engines, which can, in the matter of seconds or minutes, greatly alter a satellite's orbit. Certain more modern propulsion systems, such as electric rocket engines, are somewhat of an exception; this technicality will be discussed in further sections.

Orbital maneuvers are necessary in all stages of a satellite's lifecycle. In the beginning of a mission, the satellite is released by the launch vehicle in an orbit that is usually not the mission's orbit. Therefore, an *injection maneuver* is necessary to bring the satellite into an operational orbit. This is usually the biggest maneuver a satellite must execute during its lifecycle, consuming a high fraction of its propellant storage.

During a mission, the satellite must perform sporadic *maintenance maneuvers*, which are small course correction maneuvers to mitigate external perturbations such as atmospheric drag, Earth's oblateness effects (if undesired), gravitational attraction of celestial bodies, and solar radiation pressure. Their frequency and magnitude vary depending on mission requirements, and in industrial applications, other mission requirements must be taken into account when planning maneuvers. The presence of sensitive sensors that must not be pointed at the Sun, solar panels that must always be illuminated, or events such as observation of a ground target are examples of sources of constraints on when maneuvers can be executed. Those are by far the most common type of maneuver, and a loose, non-exhaustive classification arises naturally.

The simplest type of maneuver is that of *orbit raising*, which consists in bringing the satellite from a (often near-circular) orbit and increasing its semimajor-axis (and thus,



its period) until a desired value. This maneuver is commonly found in Low Earth Orbit (LEO) applications, due to the presence of atmospheric drag; notably, it is performed by the International Space Station (ISS) about once a month (NASA, 2009). From a theoretical standpoint, it presents a simple, introductory case, often restricted to two dimensions instead of three. There are plenty of theoretical results about it, most notably the Hohmann transfer (CHOBOTOV, 2002), a two-impulse maneuver which is known to be the two-impulse optimal from a plethora of theoretical tools. Other more elaborate results include the bielliptic transfer (CHOBOTOV, 2002), which can be shown to surpass Hohmann’s performance in certain conditions by allowing a third impulse. Another scenario that falls under this category is that of high orbit injections, such as LEO to Geostationary Earth Orbit (GEO) or LEO to Medium Earth Orbit (MEO).

A second type of maneuver is a *plane change* maneuver (CURTIS, 2020). Satellites move (approximately) in a plane which contains its position and velocity vectors and the center of Earth. By changing the direction of the velocity, this plane may be change. Common cases include an inclination change during orbital insertion, which may be required if the inclination of the target orbit is different to the latitude of the launch center (CURTIS, 2020). Another plane change instance is that of a change in the right ascension of the ascending node (RAAN), which is especially useful for Sun Synchronous Orbits (SSO). SSO injection requires that the orbit be placed approximately perpendicular to the Sun; this requires careful positioning of the ascending node. Another interesting case is that of a combined plane change and orbit raising maneuver, such as that starting from an inclined LEO orbit targeting a GEO (equatorial) orbit. A clever combination of both requirements can allow for great performance gains as compared to sequential maneuvers.

A final type of maneuver is the *phasing* maneuver (CURTIS, 2020). This maneuver consists in changing the position occupied by the satellite within the same orbit at a certain time. This maneuver is very important for *orbital rendez-vous*, where not only it is required that two vessels share the same orbit, but also they must have the same position and velocity at the same time. The execution of such a maneuver usually involves placing the satellite in an intermediate orbit with slightly different period than the initial one, and waiting multiple revolutions for the convergence of the satellite and the (mobile) target. A notable, recurring example of rendez-vous is that between the Soyuz capsule and the ISS, which requires agreement of all orbital elements and the correct phasing. This is usually a multi-revolution maneuver but recent advances have greatly reduced the time required for the rendez-vous (PARADISO, 2025).

Finally, at the end-of-life, there are legal constraints on where a satellite may be disposed of. NASA LEO missions have a deadline of 25 years for deorbiting into Earth’s atmosphere (AERONAUTICS; ADMINISTRATION, 2021), while GEO satellites are usually placed into a cemetery orbit which does not intersect the highly prized GEO region. As

an end-of-life procedure, feasibility is of utmost importance, while ensuring optimality increases the lifespan of the mission.

## 1.1 Problem statement

The central question of this work is how to find the most efficient sequence of impulsive maneuvers that take a satellite from an initial orbit to a final orbit in a given amount of time. Here, most efficient is defined as least propellant consumption. Although this problem has many known answers for particular cases, such as the Hohmann transfer, the bielliptic transfer, and some out-of-plane maneuvers (CHOBOTOV, 2002), this work aims to answer, or at least give a general procedure for answering, this question without further assumptions on the characteristics of the orbits.

An important aspect of this problem is the time taken in the transfer. Although most analytical results do not explicitly depend on time, real world problems have temporal constraints, and the mathematical treatment of dynamical systems is inherently time-dependent. Thus, characterizing possible trade-offs between time of transfer and propellant consumption is of great practical interest. Also, most tools (primer vector theory) for orbital maneuvering take the transfer time as a hyper-parameter not subject to optimization (CONWAY, 2010). Discovering whether this parameter can be estimated, optimized, or at least characterized by a feasible range is a novel approach that may prove fruitful, and therefore shall be investigated in this work.

A final topic to be explored is the question of how many impulses are needed for a particular transfer. This is the most classic question in the field, but still a topic of research. A variety of methods are given in the literature, ranging from analytical necessary conditions (LUO *et al.*, 2010), treatment of the problem as a spacecraft with thrust of infinite magnitude (TAHERI; JUNKINS, 2019), but there is no definite method for this. The possibility of other methods, such as application of discrete (combinatorial) optimization techniques, such as simulated annealing (PRESS *et al.*, 2007), can be studied and provide insight into the question at hand.

## 1.2 Hypotheses

The impulsive maneuver optimization problem is expected to be reducible to a simple parameter optimization problem where impulse parameters are directly optimized in modern non-linear optimizers, which are capable of handling thousands of constrained variables (WÄCHTER; BIEGLER, 2006). The need for numerical solutions is well established and taken as granted. However, it is expected that many local optima are to be

found, due to the non-convex nature of direct optimal control problems and of the domain of the state vector, and the periodic motion of satellites, which makes multi-revolution transfers particularly challenging.

The time of transfer is always treated as a fixed input parameter, both in the theory (CONWAY, 2010) and in reasearch (LION; HANDELSMAN, 1968). Some research suggests allowing for really long time frames, which are certainly bigger than the optimal transfer time, to allow for its detection. However, the longer the transfer time, the more revolutions around the central body are expected, which poses numerical issues. No good solution for this problem is known.

Primer vector theory is expected to be useful for determining how many impulses are necessary, up to the question of whether a solution that satisfies the necessary conditions is actually an optimum. The problem is known to have many local optima (LUO *et al.*, 2010), but it is expected that in many cases, primer vector theory can at least improve a given suboptimal solution by adding or removing impulses (CONWAY, 2010).

Finally, due to the existence of many suboptimal solution, and the expected usage of local optimizers, it is expected that solutions will be locally optimal with no guarantee of global optimality. Ensuring global optimality is a much harder problem and, except in particular cases where physical reasoning may give insight, good local optima will be accepted as solutions.

### 1.3 Objectives

The objective of this work is to describe a method capable of finding the sequence of impulses that transfer a satellite from an arbitrary starting orbit to an arbitrary final orbit. Given an initial orbital state, a final orbital state, and a transfer time, the goal is to characterize the control history that optimally satisfies theses requirements, spending the least amount of propellant possible. Secondary objectives include:

- Apply primer vector theory to the solutions found. This is a central tool in the field, and provides analytical necessary conditions for verifying optimality;
- Study how much time is needed to execute the proposed transfers;
- Compare some of the numerical results with known analytical results, namely the Hohmann transfer;
- Discuss some instances of application of this method to common aerospace scenarios;
- **Optional:** expand the work to continuous thrust propulsive models;

- **Optional:** include orbital perturbations, most notably oblateness effects.

## 1.4 Justification

The strict performance requirements in the space domain make it paramount to use orbital resources sparingly. Optimization of orbital maneuvers increases the envelope of possible missions, be it in terms of mission lifespan, which increases profitability, or in terms of mission design, allowing for bolder, high-profile missions.

In the context of Brazil's space industry, ITASAT-2 is a formation-flying mission which is subject to orbital disturbances, such as atmospheric drag and oblateness effects (FRANCO; SANTOS, 2020). Thus the need for efficient orbital maneuvers arises.

## 1.5 Work structure

This work is organized in chapters as follows:

1. Introduction, where preliminary contextualization is given;
2. Theory and fundamentals, where the mathematical description of the problem is given;
3. Bibliographic review, where some previous results in the field are discussed;
4. Methodology, where implementation details are given;
5. Preliminary and expected results, where some baseline results are exposed, and future, expected results are enumerated;
6. Planning, where a timeline of future work is given.

## 2 Theory and fundamentals

This work relies on optimal control theory and orbital mechanics. Certain tools from optimal control theory are necessary to analyze the conditions for a control trajectory to be the best according to some criterion, and under some mathematical conditions. This theory applies to a wide range of linear and non-linear systems, independently of the specifics of a dynamical system. However, this work focuses its application to one particular system: that of a body gravitationally attracted by a much more massive central body, which is the domain of orbital mechanics. Both theories will be introduced.

### 2.1 Optimal Control

Optimal control is the area of control theory which tries to find the best control action to satisfy some requirements, such as altering a system's state in some desired way. Here, "best" is defined as maximizing or minimizing some performance metric. In practice, and in particular in the scope of this work, this can be interpreted as attaining a target orbit in a certain amount of time, while minimizing fuel consumption.

The mathematical nature of an optimal control problem varies greatly depending on the nature of the system, the requirements, and the objective. Here, a selected subset of this vast theory shall be presented. Suppose a continuous time dynamical system operating on times  $t \in [0, t_f]$ , where  $t_f \in \mathbb{R}$ , given by

$$\dot{\mathbf{x}}(t) = f(\mathbf{x}(t), \mathbf{u}(t)) \quad (2.1)$$

where  $\mathbf{x}(t) : \mathbb{R} \rightarrow \mathbf{x} \subset \mathbb{R}^n$  is the state vector trajectory describing the system state,  $\mathbf{u}(t) : \mathbb{R} \rightarrow \mathbb{R}^m$  is the control vector trajectory and  $f : \mathbb{R}^n \times \mathbb{R}^m \rightarrow \mathbb{R}^n$  is the function describing its temporal dynamics.

In addition, the control vector might be subject to some inequality constraints, representing for instance saturation of actuators. Therefore, an admissible control set  $\mathcal{U}$

is defined by a vector of constraint functions  $\mathbf{g}(\mathbf{u})$  as

$$\mathcal{U} = \{\mathbf{u} \in \mathbb{R}^m \mid \mathbf{g}(\mathbf{u}) \leq 0\} \quad (2.2)$$

where the inequality is understood to hold component-wise.

At the initial time, the system is supposed to be in a given state  $\mathbf{x}_i$  such that

$$\mathbf{x}(0) = \mathbf{x}_i. \quad (2.3)$$

At the final time  $t_f$ , some components of the final state vector are specified, while others are subject to optimization. Let the index set  $\mathcal{K}$  be the set of state variables that are fixed at the final time, such that

$$\mathbf{x}^k(t_f) = \mathbf{x}_f^k, k \in \mathcal{K}, \quad (2.4)$$

where  $\mathbf{x}^k$  denotes the  $k$ -th component of  $\mathbf{x}$ , for some given values  $\mathbf{x}_f^k$ .

To complete the optimal control problem, a performance metric needs to be introduced. In general, any functional of the form  $J[\mathbf{x}(t), \mathbf{u}(t)]$  may be taken as this performance metric; however, a common form which shall be adopted in this work, is given by

$$J[\mathbf{x}(t), \mathbf{u}(t)] = h(\mathbf{x}(t_f)) + \int_0^{t_f} L(\mathbf{x}(t), \mathbf{u}(t))dt \quad (2.5)$$

where the functions  $h(\mathbf{x})$  and  $L(\mathbf{x}, \mathbf{u})$  are respectively called the *terminal cost* and the *temporal cost* functions (BERTSEKAS, 1995).

The optimal control problem is then that of finding a control trajectory  $\mathbf{u}(t)$  that minimizes (or maximizes) the performance metric. Here the problem shall be presented as a minimization problem; but the formulation is perfectly analogous for a maximization problem. That said, the complete optimal control problem may be stated as finding the function  $\mathbf{u}(t)$  such that (BRYSON; HO, 1975)

$$\mathbf{u}(t) = \arg \min_{\mathbf{u}(t), \mathbf{x}(t)} J[\mathbf{x}(t), \mathbf{u}(t)] \quad (2.6)$$

subject to

$$\dot{\mathbf{x}}(t) = f(\mathbf{x}(t), \mathbf{u}(t)) \quad (2.7)$$

$$\mathbf{x}(0) = \mathbf{x}_i \quad (2.8)$$

$$\mathbf{x}^k(t_f) = \mathbf{x}_f^k, k \in \mathcal{K}. \quad (2.9)$$

In general, this is a very hard problem. The optimization variable  $\mathbf{u}(t)$  is not merely a vector of parameters but a whole trajectory of them; thus, the search space is enormous. There are techniques to turn this problem into a simple parameter optimization problem, which are known as *direct methods* (CONWAY, 2010), which shall be discussed later. There are however tools for extracting necessary conditions for the solution of this problem at all points in time. These are known as *indirect methods*.

One of this tools is the Hamiltonian (CONWAY, 2010), a quantity that describes the ensemble of objectives and constraints. It shall be defined for a minimization problem, and maximization problems can be adapted by changing the sign of the performance metric. Given a system of the form in Equation (2.1), constraints in the forms of Equations (2.3) and (2.4), and a cost function in the form (2.5), the Hamiltonian  $H$  is defined as (BERTSEKAS, 1995)

$$H(\mathbf{x}(t), \mathbf{u}(t), \lambda(t)) = L(\mathbf{x}, \mathbf{u}) + \lambda(t)^T f(\mathbf{x}, \mathbf{u}) \quad (2.10)$$

for all times  $t$ , state and control vectors  $\mathbf{x}$  and  $\mathbf{u}$  along a trajectory.  $\lambda(t)$  is the costate trajectory, a new set of variables introduced as the continuous-time equivalent of Lagrangian multipliers. These new variables are subject to the adjoint equations

$$\dot{\lambda} = - \left( \frac{\partial H}{\partial \mathbf{x}} \right)^T = - \left( \frac{\partial f}{\partial \mathbf{x}} \right)^T \lambda - \left( \frac{\partial L}{\partial \mathbf{x}} \right)^T \quad (2.11)$$

and boundary conditions (BRYSON; HO, 1975)

$$\lambda^k(t_f) = \frac{\partial h(\mathbf{x}(t_f))}{\partial \mathbf{x}^k}, k \notin \mathcal{K}. \quad (2.12)$$

An important property of the Hamiltonian for fixed-time problems is that its value is constant with respect to time along the optimal trajectory (BERTSEKAS, 1995). For an optimal trajectory  $\mathbf{x}^*(t)$ ,  $\mathbf{u}^*(t)$ ,  $\lambda^*(t)$ , and some value  $C \in \mathbb{R}$ ,

$$H(\mathbf{x}^*(t), \mathbf{u}^*(t), \lambda^*(t)) = C, \forall t \in [0, t_f] \quad (2.13)$$

To complete the Hamiltonian approach, Pontryagin's Minimum Principle (BERTSEKAS, 1995) is introduced. It states that a necessary condition for attaining the minimum in Equation (2.6) is that, at all times  $t$ , and along the optimal trajectory,

$$\mathbf{u}^*(t) = \arg \min_{\mathbf{u} \in \mathcal{U}} H[\mathbf{x}(t), \mathbf{u}, \lambda(t)]. \quad (2.14)$$

With the control trajectory obtained as a function of  $\mathbf{x}(t)$  and  $\lambda(t)$  from Equation (2.14), there are  $2n$  variables, the state and costate trajectories, and  $2n$  bound-

ary conditions, the initial states, some final states and some final costates according to Equations (2.4) and (2.12). Thus, the problem is well-posed and configures a Two Point Boundary Value Problem (TPBVP) (BRYSON; HO, 1975).

## 2.2 Orbital Mechanics

Orbital mechanics concerns itself with the motion of bodies in space subject to gravitational and disturbance forces. A variety of models exist, differing in precision and availability of analytical tools. The simpler the model, the more analytical tools are available, and the smaller the precision. The simplest model of all, and the basis for all others, is the two body problem, where a central massive body is supposed to be stationary while a moving satellite is subject to its gravitational attraction, also known as Keplerian motion.

### 2.2.1 Two Body Motion

Let  $\mathbf{r}$  be the 3-dimensional position of a satellite, and  $\mu$  the gravitational parameter of the central body. The dynamics of the satellite's position are given by (CURTIS, 2020)

$$\ddot{\mathbf{r}} = g(\mathbf{r}) = -\frac{\mu}{\|\mathbf{r}\|^3}\mathbf{r}, \quad (2.15)$$

where  $g(\mathbf{r})$  represents the gravitational acceleration field, thus configuring a 6-dimensional state vector  $\mathbf{x} = \begin{bmatrix} \mathbf{r}^T & \mathbf{v}^T \end{bmatrix}^T$ , where  $\mathbf{v}$  is the satellite's velocity. The system contains a singularity at the states with  $\|\mathbf{r}\| = 0$ , which configures a non-convex domain. In practice, this point is rarely encountered as it lies inside of the central body, thus far from the regions of interest. It is proven that no analytical solution exists for this differential equation; however, much is known about its solutions.

In this model, the possible trajectories are known to be conics, and therefore restricted to a plane. For bound satellites, that is, those in orbit around the central body, this trajectory is an ellipse where the central body lies on one of its foci. Mathematically, a “bound” satellite is one whose specific energy (mechanical energy over mass of the satellite), given by (CURTIS, 2020)

$$\epsilon = -\frac{\mu}{\|\mathbf{r}\|} + \frac{\mathbf{v}^2}{2}, \quad (2.16)$$

is negative. The trajectory is closed, and the movement is periodic with period (CURTIS,



2020)

$$T = 2\pi\sqrt{\frac{a^3}{\mu}} \quad (2.17)$$

where  $a$  is the semi-major axis of the ellipse.

In this case, an alternative state vector may be introduced in the form of the Keplerian elements. These are (CURTIS, 2020):

- $a$ : semi-major axis of the ellipse;
- $e$ : excentricity of the ellipse;
- $i$ : inclination of the orbit's plane with respect to the equatorial plane;
- $\Omega$ : right ascension of the ascending node, that is, angle between the vernal equinox direction and the direction where the satellite crosses the equatorial plane from South to North;
- $\omega$ : argument of perigee, or angle, in the plane of the orbit, between the ascending node and the perigee (point of smallest distance to the central body);
- $\theta$ : true anomaly, or angle between the perigee and the current position of the satellite.

These elements are related to the Cartesian state vector through the geometric description of a point on an ellipse, rotated through the Euler angles  $\Omega$ ,  $i$ ,  $\omega$  (CURTIS, 2020).

In this formulation, only the true anomaly is a function of time, all other elements being constant. The true anomaly can be related to time implicitly through two other quantities, the mean anomaly  $M$  and the excentric anomaly  $E$  (CURTIS, 2020):

$$M = 2\pi\frac{t - t_p}{T} \quad (2.18)$$

$$E - e \sin E = M \quad (2.19)$$

$$\tan \frac{\theta}{2} = \sqrt{\frac{1+e}{1-e}} \tan \frac{E}{2} \quad (2.20)$$

where  $t_p$  is the time of the last perigee passage. By computing the mean anomalies in an initial and a final time, and solving the notorious Kepler's Equation (2.19), and finally finding a suitable true anomaly with Equation (2.20), a semi-analytical temporal solution can be found. The process of finding the position of a satellite in the future is called *orbit*

*propagation.* Define an orbit propagator as a function  $p_o(\mathbf{x}_i, t)$  such that

$$\mathbf{x}_f = p_o(\mathbf{x}_i, t) \quad (2.21)$$

where  $\mathbf{x}_f$  is the satellite's final state after a time  $t$ , with initial state  $\mathbf{x}_i$ .

## 2.2.2 Orbital Perturbations

The two body model is an idealized model amenable to analytical solutions, which neglects many real world phenomena. In LEO, the most important perturbations are oblateness effects (J2) and atmospheric drag (CURTIS, 2020), which are introduced ahead.

### 2.2.2.1 Oblateness effects

The Earth being an oblate spheroid, its gravity field is not perfectly central, neither does it behave like the inverse square law predicted by the two body model. Instead, the Earth's geopotential is modeled as a point mass potential plus spherical harmonics terms with coefficients subject to empirical fitting. The biggest non-sphericity of Earth is its oblateness, the increased width at the Equator. This effect is described by the coefficient  $J_2$ , which causes a perturbing acceleration  $\mathbf{a}_{J_2}$  given by

$$\mathbf{a}_{J_2} = \frac{3J_2\mu R^2}{2r^4} \begin{bmatrix} \frac{x}{r} \left( 5\frac{z^2}{r^2} - 1 \right) \\ \frac{y}{r} \left( 5\frac{z^2}{r^2} - 1 \right) \\ \frac{z}{r} \left( 5\frac{z^2}{r^2} - 3 \right) \end{bmatrix}, \quad (2.22)$$

where  $R$  is Earth's Equatorial radius.

Thus, this model's dynamics can be expressed solely as a function of the position, since it is a conservative model:

$$\ddot{\mathbf{r}} = g_{J_2}(\mathbf{r}) = -\frac{\mu}{r^3}\mathbf{r} + \mathbf{a}_{J_2}. \quad (2.23)$$

### 2.2.2.2 Atmospheric Drag

Atmospheric drag affects satellites in LEO by generating a force opposed to the relative velocity of the satellite w.r.t. the Earth's atmosphere, which rotates with it. The drag force is proportional to atmospheric density  $\rho(r)$ , as a function of the satellite's distance to Earth. Modelling this dependence is not a trivial task, with accurate models taking solar activity and Earth's temperature into account. A simple model is given by the US Standard Atmosphere 1976, which gives empirical coefficients  $\rho_i$  and  $H_i$ , valid for height

intervals  $[h_i, h_i + 1]$ , for  $i = 1, \dots, 28$ . Then, atmospheric density is given piecewise by

$$\rho(r) = \rho_i \exp\left(-\frac{(r - (h_i + R))}{H_i}\right), \quad (2.24)$$

where  $i$  is such that  $h_i \leq r - R \leq h_{i+1}$ . The satellite is parameterized by a reference surface  $S$ , drag coefficient  $C_D$  and mass  $m$ . Considering that the Earth rotates with angular velocity  $\omega_E$ , the relative velocity of the satellite w.r.t. the atmosphere is given by

$$\mathbf{v}_r = \mathbf{v} - (\omega_E \hat{\mathbf{z}}) \times \mathbf{r}. \quad (2.25)$$

Finally, the acceleration due to drag  $\mathbf{a}_D$  is given by

$$\mathbf{a}_D = -\frac{1}{2}\rho(r)\frac{SC_D}{m}\|\mathbf{v}_r\|\mathbf{v}_r, \quad (2.26)$$

which can be added as a perturbing non-conservative acceleration to the model.

### 2.2.3 Lambert's Problem

An important problem in orbital mechanics is that of the determination of the initial and final velocities of a satellite that passes through two points in space  $\mathbf{r}_1$  and  $\mathbf{r}_2$  with a time interval  $\Delta t$  in between, as illustrated in Figure 2.1. This problem first arose in the field of orbit determination but also finds application in the context of orbital maneuvers. Namely, Lambert's Problem seeks to find a feasible solution to a TPBVP, which is of interest to the optimal control TPBVP.

This problem suffers from a physical indetermination in the case of collinear  $r_1$  and  $r_2$ : the plane of the orbit is indeterminate. In this case, one can find many feasible solutions but determining exact velocities requires extra information about the plane of the orbit.

In general, this problem can have multiple solutions, corresponding to prograde and retrograde trajectories, with less than one or multiple revolutions. The resulting orbit can, in general, be elliptic, parabolic or hyperbolic. Handling this variety of solution types is not simple. A simple formulation which does not handle multiple revolutions nor the indetermination mentioned can be built with universal variables (CURTIS, 2020). Multiple revolutions and finding the radial and tangent components of the velocity in the indeterminate case can be handled with more complex algorithms (SUKHANOV, 2010). A generic, Cartesian coordinates-based algorithm is also possible, as will be discussed in Chapter 4.



is required to maneuver to an orbital state  $\mathbf{x}_f$  in a time  $t_f$ , and it is desired to minimize the amount of propellant used. A convenient way of expressing this is to maximize the final mass of the spacecraft, with constraints:

$$\max_{\mathbf{F}(t)} m(t_f) \quad (2.28)$$

$$\mathbf{x}(0) = \mathbf{x}_i \quad (2.29)$$

$$\mathbf{x}(t_f) = \mathbf{x}_f \quad (2.30)$$

### 2.3.1 Constant specific impulse model

Chemical and cold gas thrusters are characterized by an exhaust velocity  $v_e$  at which the propellant flow is ejected from the spacecraft. With a propellant flow rate  $\dot{m}_p$ , the thrust  $\mathbf{F}$  is given by

$$\|\mathbf{F}\| = v_e \dot{m}_p \quad (2.31)$$

The propellant flow is deducted from the spacecraft's mass; therefore it can be stated that  $\dot{m} = -\dot{m}_p$ . Thus, in this model, the spacecraft's mass is a seventh state variable. A new state vector  $\mathbf{x}_m = [\mathbf{r}^T \quad \mathbf{v}^T \quad m]^T$  is defined and subject to the dynamics

$$\begin{bmatrix} \dot{\mathbf{r}} \\ \dot{\mathbf{v}} \\ \dot{m} \end{bmatrix} = \begin{bmatrix} \mathbf{v} \\ -\frac{\mu}{\|\mathbf{r}\|^3} \mathbf{r} + \frac{\mathbf{F}}{m} \\ -\frac{\|\mathbf{F}\|}{v_e} \end{bmatrix} \quad (2.32)$$

In addition, thrusters have limited flow rates, which imposes a maximum thrust magnitude  $F_{\max}$ :

$$\|\mathbf{F}\| \leq F_{\max} \quad (2.33)$$

The objective from Equation (2.28) can be developed for this model by integrating  $\dot{m}$  as

$$m(t_f) = m(0) - \int_0^{t_f} \frac{\|\mathbf{F}\|}{v_e} dt \quad (2.34)$$

Let  $\mathbf{\Gamma}$  be the acceleration due to thrust such that  $\mathbf{\Gamma} = \frac{\mathbf{F}}{m}$ . The literature (CONWAY, 2010) then suggests considering that the propellant consumption is small compared to the total mass of the satellite, such that it can be stated that

$$m(t_f) \approx m(0) - \frac{m(0)}{v_e} \int_0^{t_f} \|\mathbf{\Gamma}\| dt \quad (2.35)$$

Therefore the objective can be restated as

$$\min_{\Gamma(t)} \int_0^{t_f} \|\Gamma\| dt \quad (2.36)$$

subject to  $\|\Gamma(t)\| \leq \Gamma_{\max}$  at all times, with  $\Gamma_{\max} = \frac{F_{\max}}{m(0)}$ .

If the control variable is set to be  $\Gamma$  instead of  $\mathbf{F}$ , this leads to a mass-independent problem. This approximation leads to primer vector theory, and is therefore important.

### 2.3.2 Impulsive propulsion model

A very simple propulsion model that allows for easier solution of the orbital maneuvering problem supposes that the propulsive forces are much greater and operate much faster than the gravitational force, introducing discontinuities in velocity. This is called *impulsive thrust*. The propulsion model relies on Tsiolkovsky's Equation (CONWAY, 2010),

$$\Delta v = v_e \ln \left( \frac{m_i}{m_f} \right), \quad (2.37)$$

where  $\Delta v$  is the magnitude of an instantaneous change in velocity,  $v_e$  is the engine's exhaust velocity (which is treated as a known parameter),  $m_i$  is the initial spacecraft mass and  $m_f$  is the final mass. Supposing a burn happens at time  $t_b$ , the propulsion model can then be expressed through a Dirac delta as

$$\left. \frac{F}{m} \right|_{t=t_b} = \delta(t - t_b) v_e \ln \left( \frac{m(t_b^-)}{m(t_b^+)} \right) = \delta(t - t_b) \Delta v, \quad (2.38)$$

which yields a velocity discontinuity

$$\|\mathbf{v}(t_b^+) - \mathbf{v}(t_b^-)\| = v_e \ln \left( \frac{m(t_b^-)}{m(t_b^+)} \right) = \Delta v. \quad (2.39)$$

Now, between impulses there are coasting arcs where the vessel is subject only to external (gravitational) forces, as illustrated in Figure 2.2. Considering a generic maneuver with  $n$  burns, there are  $n + 1$  coasting segments related by the change in velocity  $\Delta \mathbf{v}_j$  associated with the  $j$ -th burn. Considering burn times  $t_j$ , with  $t_f \geq t_{j+1} \geq t_j \geq 0$ , and

the initial and final times 0 and  $t_f$ , the system is subject to boundary conditions

$$\mathbf{x}(0) = \mathbf{x}_i \quad (2.40)$$

$$\mathbf{r}(t_j^+) = \mathbf{r}(t_j^-), \quad \forall j = 1, \dots, n \quad (2.41)$$

$$\mathbf{v}(t_j^+) = \mathbf{v}(t_j^-) + \Delta \vec{v}_j, \quad \forall j = 1, \dots, n \quad (2.42)$$

$$\mathbf{x}(t_f) = \mathbf{x}_f \quad (2.43)$$

and to dynamical Equation (2.15) in the intermediate times. Using the concept of orbit propagator, this adds the constraints

$$\mathbf{x}(t_1^-) = p_o(\mathbf{x}(0), t_1) \quad (2.44)$$

$$\mathbf{x}(t_{j+1}^-) = p_o(\mathbf{x}(t_j^+), t_{j+1} - t_j), \forall j = 1, \dots, n-1 \quad (2.45)$$

$$\mathbf{x}(t_f) = p_o(\mathbf{x}(t_n^+), t_f - t_n) \quad (2.46)$$

to the previous list. Each impulse is described by its time  $t_j$  and its velocity change vector  $\Delta \mathbf{v}_j$ . Accounting for  $\mathbf{x}(0)$ , all of the intermediate  $\mathbf{r}(t_j^-)$ ,  $\mathbf{r}(t_j^+)$ ,  $\mathbf{v}(t_j^-)$  and  $\mathbf{v}(t_j^+)$ , and also the final state  $\mathbf{x}(t_f)$ , plus the impulse parameters, there are  $6 + 12n + 6 + 4n = 16n + 12$  unknowns. At the same time, there are  $6 + (3 + 3)n + 6 + 6 + 6(n-1) + 6 = 12n + 18$  constraints. Therefore, for general initial and final conditions, the *minimal number of impulses* is 2.

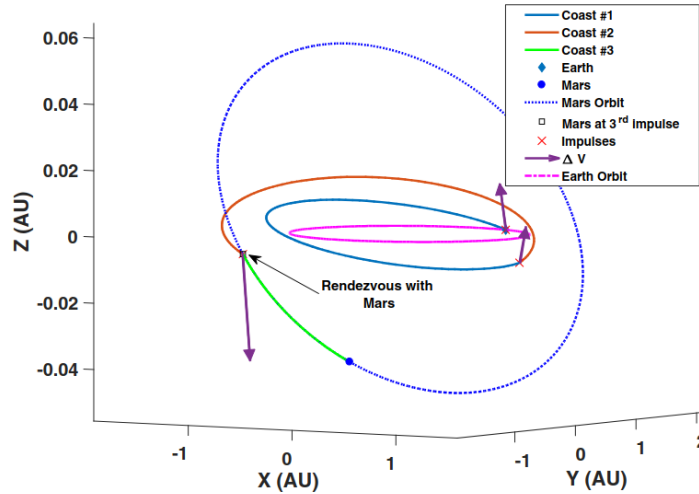


FIGURE 2.2 – illustration of impulsive transfer with Earth to Mars transfer in 3 impulses. Source: (TAHERI; JUNKINS, 2019).

Tsiolkovsky's equation can be applied to all impulses, thus relating the final and initial masses with the total velocity change, which is the sum of all  $n$  burns executed during the transfer:

$$m(t_f) = m(0) \exp \left( - \frac{\sum_{i=1}^n \Delta v_i}{v_e} \right) \quad (2.47)$$

Since  $v_e$  and  $m(0)$  are not subject to optimization, the objective (2.28) is equivalent to minimizing the sum of magnitudes of impulses used during the transfer:

$$\min \sum_{i=1}^n \Delta v_i. \quad (2.48)$$

Thus, in the impulsive case, the problem is *independent of spacecraft mass*, and it can be eliminated from the state vector. However, the control trajectory  $\mathbf{\Gamma}(t)$  in the impulsive case is not a function, but a *measure*. It therefore needs to be implemented not as a function of time, as usual in optimal control, but as magnitudes of discontinuities in the state trajectory. This introduces the number of allowed impulses as an optimization hyperparameter (LEANDER *et al.*, 2015). To choose an optimal number of impulses, the theory of primer vectors (see ahead) can help determine the number of impulses needed (LUO *et al.*, 2010).

### 2.3.2.1 Hohmann transfer

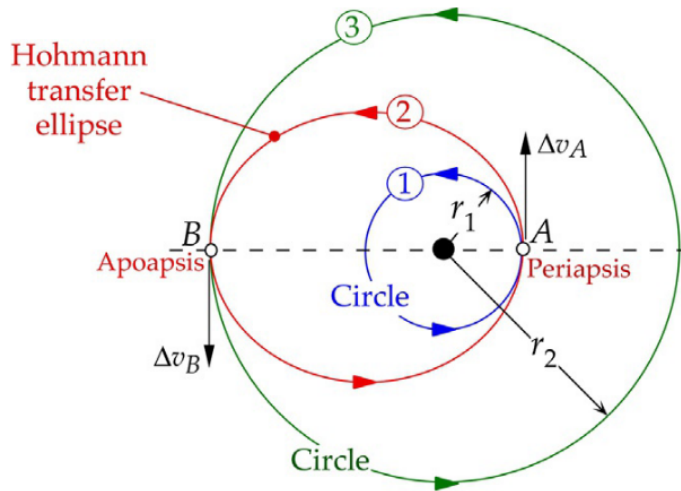


FIGURE 2.3 – Hohmann transfer diagram. Source: (CURTIS, 2020)

The prototypical orbital maneuver case is that of a two-impulse transfer between two coplanar circular orbits in Keplerian dynamics (CHOBOTOV, 2002). The intermediate orbit, between the two impulses, is an ellipse that is tangent to both initial and final orbits, as can be seen in Figure 2.3. This transfer has a known analytical optimal, which can be proven by several different methods. Some useful quantities relating to this transfer are given in the following. Given an initial circular orbit of semi-major axis  $a_1$  and a final circular orbit with semi-major axis  $a_2$ , the total change in speed required is equal



to (CHOBOTOV, 2002):

$$\sum \|\Delta \mathbf{v}\| = \sqrt{\mu \left( \frac{2}{a_1} - \frac{2}{a_1 + a_2} \right)} - \sqrt{\frac{\mu}{a_1}} + \sqrt{\frac{\mu}{a_2}} - \sqrt{\mu \left( \frac{2}{a_2} - \frac{2}{a_1 + a_2} \right)} \quad (2.49)$$

The transfer time is half of the transfer orbit's period. With  $t_H$  being the Hohmann transfer duration, is given by (CHOBOTOV, 2002)

$$t_H = \pi \sqrt{\frac{\left( \frac{a_1 + a_2}{2} \right)^3}{\mu}}. \quad (2.50)$$

## 2.4 Primer vector theory

The application of optimal control theory to orbital maneuvers dates back to the 1960s, with pioneering work by Lawden (CONWAY, 2010). In particular, he coined the term "primer vector" as an analogy with the fact that the costate trajectory imposes a necessary condition for firing the engines, thus acting as a "primer". This theory is based on the indirect necessary conditions provided by the Hamiltonian formalism previously exposed, and is explored in Conway (2010). Here, the impulsive thrust case will be treated as a limiting case of finite thrust when  $\Gamma_{\max} \rightarrow \infty$ .

### 2.4.1 Conservative Orbital model

Firstly, a model where  $\ddot{\mathbf{r}} = g(\mathbf{r}) = \nabla \Phi(\mathbf{r})$ , where  $\Phi(\mathbf{r})$  is a gravitational potential field, is considered. This type of model contains the two body approach as well as the J2 model.

The acceleration due to the thrust  $\mathbf{\Gamma}$  can be split into its magnitude and direction as  $\mathbf{\Gamma} = \Gamma \hat{\mathbf{u}}$ ,  $\Gamma = \|\mathbf{\Gamma}\|$ ,  $\|\hat{\mathbf{u}}\| = 1$  so that the objective from Equation (2.36) can be rewritten as

$$\min_{\Gamma(t), \hat{\mathbf{u}}(t)} \int_0^{t_f} \Gamma dt \quad (2.51)$$

and the Hamiltonian of the system is the given by

$$H = \Gamma + \begin{bmatrix} \lambda_r^T & \lambda_v^T \end{bmatrix} \begin{bmatrix} \mathbf{v} \\ g(\mathbf{r}) + \Gamma \hat{\mathbf{u}} \end{bmatrix} \quad (2.52)$$

The costate is subject to the adjoint equations given in block matrix form as

$$\begin{bmatrix} \dot{\lambda}_r \\ \dot{\lambda}_v \end{bmatrix} = \begin{bmatrix} 0_{3 \times 3} & -\left( \frac{\partial g(\mathbf{r})}{\partial \mathbf{r}} \right)^T \\ -I_{3 \times 3} & 0 \end{bmatrix} \begin{bmatrix} \lambda_r \\ \lambda_v \end{bmatrix} \quad (2.53)$$

which is linear in the costate variables. For problems with final position and velocity constraints, no boundary conditions are given for the adjoint equations.

Rearranging the Hamiltonian to factor  $\Gamma$ ,

$$H = (1 + \lambda_v^T \hat{\mathbf{u}})\Gamma + \lambda_r^T \mathbf{v} + \lambda_v^T g(\mathbf{r}). \quad (2.54)$$

By applying Pontryagin's Minimum Principle, the thrust magnitude  $\Gamma$  is given piecewise by analyzing the sign of its coefficient:

$$\Gamma = \begin{cases} \Gamma_{\max} & , 1 + \lambda_v^T \hat{\mathbf{u}} < 0 \\ 0 & , 1 + \lambda_v^T \hat{\mathbf{u}} > 0 \\ \text{intermediate} & , \text{otherwise} \end{cases} \quad (2.55)$$

The case where  $1 + \lambda_v^T \hat{\mathbf{u}} = 0$  on a finite interval of time will not be considered here; these are *singular arcs* and occur rarely (MORELLI *et al.*, 2023). When  $\Gamma = \Gamma_{\max}$ , its coefficient should be as negative as possible, which happens when  $\hat{\mathbf{u}}$  has the opposite direction to  $\lambda_v$ :

$$\hat{\mathbf{u}} = -\frac{\lambda_v}{\|\lambda_v\|}. \quad (2.56)$$

This direction, the *optimal thrust direction* given by  $-\lambda_v$  is what constitutes the primer vector  $\mathbf{p}$ , which is defined as

$$\mathbf{p} = -\lambda_v. \quad (2.57)$$

The engine firing conditions can be stated solely as a function of the primer vector as (CONWAY, 2010)

$$\Gamma = \begin{cases} \Gamma_{\max} & , \|\mathbf{p}\| > 1 \\ 0 & , \|\mathbf{p}\| < 1 \\ \text{intermediate} & , \text{otherwise} \end{cases} \quad (2.58)$$

The impulsive thrust case is then found by letting  $\Gamma_{\max} \rightarrow \infty$ , in which case the segments where  $\|\mathbf{p}\| > 1$  approach points, and the thrust cases become

$$\Gamma = \begin{cases} 0 & , \|\mathbf{p}\| < 1 \\ \Delta \mathbf{v} \delta & , \|\mathbf{p}\| = 1 \end{cases}, \quad (2.59)$$

for some (possibly null) velocity increment  $\Delta \mathbf{v}$

Alternatively, one could reason about the constant value of the Hamiltonian which, from Equation (2.13), is finite. Therefore, at the impulse instants, where  $\Gamma$  is unbounded,

its coefficient  $1 + \lambda_v^T \hat{\mathbf{u}}$  must be 0, leading to  $\hat{\mathbf{u}} = -\lambda_v = \mathbf{p}$ , and the condition  $\|\mathbf{p}\| = 1$ .

The necessary conditions offered by primer vector theory for an impulsive maneuver scenario are (CONWAY, 2010):

1.  $\mathbf{p}(t)$  and  $\dot{\mathbf{p}}(t)$  are continuous;
2.  $\|\mathbf{p}\| \leq 1$ ;
3.  $\mathbf{p} = \hat{\mathbf{u}}$  at the impulse instants, with the corollary that when an impulse happens,  $\|\mathbf{p}\| = 1$ ;
4.  $\frac{d\|\mathbf{p}\|}{dt} = 0$  at impulses between the initial and final times (non-inclusive).

#### 2.4.1.1 Primer vector trajectory calculation

From Equations (2.53) and (2.57), the primer vector differential equations are

$$\begin{bmatrix} \dot{\mathbf{p}} \\ \ddot{\mathbf{p}} \end{bmatrix} = \begin{bmatrix} \mathbf{0}_3 & \mathbf{I}_3 \\ \left[\frac{\partial g}{\partial \mathbf{r}}\right]^T & \mathbf{0}_3 \end{bmatrix} \begin{bmatrix} \mathbf{p} \\ \dot{\mathbf{p}} \end{bmatrix} = \mathbf{A}_p \begin{bmatrix} \mathbf{p} \\ \dot{\mathbf{p}} \end{bmatrix} \quad (2.60)$$

However, since  $g = \nabla\Phi = \left(\frac{\partial\Phi}{\partial\mathbf{r}}\right)^T$ ,  $\left[\frac{\partial g}{\partial\mathbf{r}}\right]$  is actually the Hessian matrix of the potential field, which is symmetric. Therefore, the primer vector is subject to the same equation as the variational perturbations in Equation TODO. Since Equation (2.60) is linear on the variables, it admits a solution through the form of a state transition matrix  $\Phi_p(t - t_0)$  such that

$$\begin{bmatrix} \mathbf{p}(t) \\ \dot{\mathbf{p}}(t) \end{bmatrix} = \Phi_p(t - t_0) \begin{bmatrix} \mathbf{p}(t_0) \\ \dot{\mathbf{p}}(t_0) \end{bmatrix}. \quad (2.61)$$

and, by analogy with the variational state transition matrix,

$$\Phi_p(t - t_0) = \frac{\partial \mathbf{x}(t)}{\partial \mathbf{x}(t_0)}. \quad (2.62)$$

This way of computing  $\Phi_p(t - t_0)$  will be termed the STM method for primer vector calculation, and is valid for all conservative force models. For the two body model in particular, a closed form for  $\Phi_p(t - t_0)$  exists (GLANDORF, 1969).

Computing the primer vector trajectory is done piecewise on coasting arcs between two consecutive impulses, since the primer vector is known at impulse times. Since  $\mathbf{p}$  is known at both ends, but not  $\dot{\mathbf{p}}$ , this configures a linear TPBVP. For two consecutive

impulses,  $\Delta v_1$  at time  $t_1$  and  $\Delta v_2$  at time  $t_2$ , the primer vector values are given by:

$$\mathbf{p}(t_1) = \frac{\Delta \mathbf{v}_1}{\|\Delta \mathbf{v}_1\|} \quad (2.63)$$

$$\mathbf{p}(t_2) = \frac{\Delta \mathbf{v}_2}{\|\Delta \mathbf{v}_2\|} \quad (2.64)$$

The state transition between these two instants can be stated as

$$\begin{bmatrix} \mathbf{p}(t_2) \\ \dot{\mathbf{p}}(t_2) \end{bmatrix} = \Phi_p(t_2 - t_1) \begin{bmatrix} \mathbf{p}(t_1) \\ \dot{\mathbf{p}}(t_1) \end{bmatrix} = \begin{bmatrix} \mathbf{M}(t_2 - t_1) & \mathbf{N}(t_2 - t_1) \\ \mathbf{S}(t_2 - t_1) & \mathbf{T}(t_2 - t_1) \end{bmatrix} \begin{bmatrix} \mathbf{p}(t_1) \\ \dot{\mathbf{p}}(t_1) \end{bmatrix} \quad (2.65)$$

where  $\mathbf{M}$ ,  $\mathbf{N}$ ,  $\mathbf{S}$  and  $\mathbf{T}$  are square matrices. From now on the times shall be denoted as indices for conciseness. If  $\mathbf{p}$  and  $\dot{\mathbf{p}}$  are known for a certain time, the entire trajectory can be found. It is easy to isolate  $\dot{\mathbf{p}}_1 = \dot{\mathbf{p}}(t_1)$ :

$$\dot{\mathbf{p}}_1 = \mathbf{N}_{21}^{-1} (\mathbf{p}_2 - \mathbf{M}_{21}\mathbf{p}_1). \quad (2.66)$$

$\mathbf{N}_{21}$  is invertible except for isolated values of  $t$  (CONWAY, 2010); in these cases, the primer vector trajectory is assumed to lie in the orbital plane, spanned by  $\begin{bmatrix} \mathbf{r}_1 & \mathbf{v}_1 \end{bmatrix}$ . Thus, for singular  $N$ ,

$$\dot{\mathbf{p}}_1 = \begin{bmatrix} \mathbf{r}_1 & \mathbf{v}_1 \end{bmatrix} (\mathbf{N}_{21} \begin{bmatrix} \mathbf{r}_1 & \mathbf{v}_1 \end{bmatrix})^\dagger (\mathbf{p}_2 - \mathbf{M}_{21}\mathbf{p}_1) \quad (2.67)$$

where  $A^\dagger$  denotes the pseudo-inverse of a rectangular matrix.

## 3 Bibliographic review

In this chapter, previous results relating to the field of orbital maneuvering are presented. Relevant research spans the 1960's all the way to recent years. In particular, results about the solution and application of the Lambert problem, usage of primer vector theory and direct optimization approaches are presented.

### 3.1 Lambert Problem

Efficient solutions to the Lambert problem have been of interest for many centuries now, and many algorithms exist, with varying convergence guarantees and indetermination handling. An algorithm based on continued fractions (BATTIN; VAUGHAN, 1984) has been proposed, and it shows promising results in terms of number of iterations until convergence. It also relies on an orbital transformation to bypass the indeterminate case, choosing one of many possible solutions. However, it requires previous knowledge of the type of orbit (elliptic, parabolic, hyperbolic) and good initial guesses for parameters with difficult physical interpretation, making it not suitable for trajectory optimization.

OTTESEN; RUSSELL (2020) present a way of applying many embedded Lambert Problems to trajectory optimization. In their approach, time is also an optimization variable. Many orbital segments of equal duration are concatenated and impulses are allowed to happen at each boundary. Then, a Cartesian variables-based Lambert problem is solved for each segment. Impulses at segment boundaries are found to be significant only at a handful of boundaries. With a big number of segments, this approximates the number, instant and magnitudes well. The Cartesian variables-based Lambert problem solution is indeed applicable to trajectory optimization, and this result also offers good insights into how to find appropriate transfer times between orbits.

## 3.2 Primer Vector theory

The evolution of the primer vector along coasting arcs is of interest for the solution of impulsive maneuvering problems. An analytical form of the state transition matrix is given in GLANDORF (1969). A clever choice of time-changing basis allows for the direct solution of the components of the primer vector differential equations (Lagrange multiplier equations), which can then be written in matrix form. The state transition matrix is given as the product of a time-evolving matrix with its inverse at the initial time; closed form expressions are given for the  $6 \times 6$  state transition matrix. Despite being restricted to the two body problem, this result proves really useful since it allows the circumvention of the solution of a TPBVP.

LION; HANDELSMAN (1968) also give a closed-form expression for the state transition matrix and a review of the application of primer vector theory. In particular, several common cases of primer vector trajectories are explored, and the relationship between suboptimal primer vector trajectories and the necessary changes is explored. Overall, Lion and Handelsman provide useful examples for understanding this theory.

Finally, an interactive algorithm for computing the optimal number of impulses based on analyzing the primer vector trajectories is given in LUO *et al.* (2010). The discrete nature of the variable “number of impulses” requires tools more powerful than continuous variable nonlinear solvers, such as evolutionary algorithms. The proposed algorithm iterates through proposing an  $n$  impulse maneuver, analyzing its primer vector history and optimizing impulse times, if needed, and then adding maneuvers if the necessary conditions are not yet satisfied. This remains one of the most direct ways of optimizing the number of impulses; however, the usage of primer vector theory provides only *necessary* conditions, which can lead to many false (or local) optima. Similar approaches are found in JEZEWSKI; ROZENDAAL (1968), which applies it to an Apollo rendezvous, with a large plane change maneuver.

## 3.3 Direct Optimization

The central question of how many impulses are needed for a maneuver is tackled through the continuous-thrust approach in TAHERI; JUNKINS (2019). A continuous thrust model is established and a sequence of increasing maximum thrust values is analyzed. Starting with the minimum thrust needed to execute the maneuver in the given time (case in which the engines fire incessantly), the thrust is continuously increased, and gaps in the thrusting times appear. In the limiting case of very high thrusts approaching infinity, engine firing closely resembles an impulse. This gives, to very good approximation, the

needed number of impulses. The main disadvantage of this approach is the need for a continuous thrust model, in addition to an impulse thrust model.

A similar approach is presented in ARYA *et al.* (2023), where a “control sweep” is performed to identify how many impulses are necessary, thus excluding the number of impulses as a problem variable. In particular, both continuous thrust constant specific impulse problems and continuous thrust variable specific impulse problems (not treated in the present work) are used during this step. These problems help in finding better optima in multi-revolution maneuvers, where multiple local optima exist. In addition, the importance of impulsive solutions is reaffirmed. Despite being abstractions, impulsive solutions provide lower bounds on fuel usages, can provide feasibility insights and can be abstracted from spacecraft mass.

The existence of multiple global optima is explored in SALOGLU *et al.* (2023), which proposes a method for generating families of transfer orbits with many impulses starting with a seed two-impulse maneuver. From a theoretical point of view, this highlights the non-convexity of the orbital maneuver optimization problem (existence of many optima), often tied to the periodicity of orbits. From a practical point of view, it exposes the concept of *phasing orbit*, an intermediate orbit between two consecutive impulses that can be chosen arbitrarily from certain period values without changing the delta-V budget. Also, the possibility of reducing flight time based on some of those solutions is also explored. However, these results are mostly applicable to long time horizon problems.

In PRUSSING; CHIU (1986), multiple impulse maneuvers for fixed time rendez-vous between spacecraft in a subclass of circular orbits is considered. The fixed time rendez-vous problem is analogous to the problem of transfer to a particular state in fixed time. Despite the restriction to a subset of possible orbits, it is shown that there is a certain minimum time required for the optimal time-open solutions (such as Hohmann transfers) to be found. Again, primer vector theory is applied but sometimes leads to local optima, and divergences from the established primer vector algorithm can sometimes be preferred over following it strictly.

## 4 Methodology

All code was implemented in the Julia language due to the availability of *packages* for subproblems of this work. In the next section, several components of the solution to the problem of optimization of impulsive maneuvers are detailed, along with its full formulation.

### 4.1 Orbit Propagation

The implementation of an orbit propagator concerns itself with the implementation of the function  $p_o(\mathbf{x}, t)$  introduced in Equation (2.21). Two different cases are to be considered: “explicit” propagation, where numerical inputs are available and a numerical output is desired; and “implicit” propagation, where the propagation step is a part of a larger solver.

Brazil’s National Institute of Space Research (INPE) developed a package for orbit propagation and analysis with several models (Kepler, J2 semi-analytical secular and short term, among others) called **SatelliteToolbox** (CHAGAS *et al.*, 2025). It provides quite convenient functions for converting between the Cartesian state vector  $\begin{bmatrix} \mathbf{r}^T & \mathbf{v}^T \end{bmatrix}^T$  and the Keplerian elements, as well as functions for the propagation of orbits by some specified amount of time  $t_p$ . Its algorithms were chosen with precision around edge cases in mind (SCHWARZ, 2014), making it numerically precise but unsuitable for nonlinear solvers, which expect differentiable functions everywhere. The functions in this package are also limited to elliptic orbits.

Therefore, this is an auxiliary package used for verification, initial guess generation, and direct numerical propagation whenever required. When propagation is required in the statement of a nonlinear optimization problem, another method for orbit propagation is required. Discretized numerical integration in Cartesian coordinates was chosen for this. Discretized integration inside a numerical solver can be done via collocation, direct shooting or multiple shooting (also known as relaxation) (PRESS *et al.*, 2007). Multiple shooting was chosen since it leads to a sparse problem, which benefits the performance of the chosen solver (see next section).



Let  $\mathbf{x}_{\text{next}} = f_{RK}(\mathbf{x}_{\text{prev}}, \Delta t)$  be the (two-body) dynamics function discretized through a fourth order Runge Kutta method. Then a number  $N$  of integration steps is chosen and  $N + 1$  state vector variables  $\mathbf{x}^j, j = 1, \dots, N + 1$  are created belonging to an array  $\chi \in \mathbb{R}^{6 \times (N+1)}$ . They are subject to the constraints

$$\mathbf{x}^{j+1} = f_{RK}(\mathbf{x}^j, \frac{t_p}{N}), j = 1, \dots, N. \quad (4.1)$$

This leaves  $\dim \mathbf{x} = 6$  degrees of freedom, which are to be specified with a boundary condition. This boundary condition can be an initial condition, a final condition or relation to another coasting segment through an impulse, as will be discussed in Section 4.6. Thus, this parameterization of orbital propagation is *isoconstrained*.

## 4.2 Optimization algorithm with fixed number of impulses

### 4.3 Primer vector algorithm

### 4.4 Nonlinear solver

Nonlinear solvers are algorithms which iteratively approximate the solution to a system of nonlinear equations or a constrained optimization problem. Many algorithms, and many different algorithms exist. Optimizer algorithms may be classed as local or global, depending on whether they find a local (best in a region) or global (best in the domain) solution; stochastic, according to the presence or absence of random seeding; and the usage of function evaluations only, gradient evaluations, or even Hessian evaluations (PRESS *et al.*, 2007). All local methods require an initial guess as input.

Of interest to this work are deterministic local gradient-based algorithms. They are well suited to nonlinear (but continuous and differentiable) problems with continuous variables subject to nonlinear constraints. By exploiting the gradient, faster algorithms are available. The choice for a local, deterministic solver comes from the fact that these algorithms have much faster convergence than global stochastic algorithms such as simulated annealing. To make up for the loss of global optimality, good initial guesses must be supplied.

Julia offers a multitude of nonlinear solvers, each with different scope, interface, and algorithms. This work has chosen to use JuMP (LUBIN *et al.*, 2023), a package which offers a modelling language for optimization problems that is quite close to mathematical notation. The package's *tech stack* can be seen in Figure 4.1. Internally, JuMP relies on an intermediary package, MathOptInterface, which standardizes solver interfaces. This

in turn allows for the usage of `Ipopt_jll`, an unofficial wrapper for the Ipopt solver. Ipopt is an open-source nonlinear solver widely recognized for its speed and precision, outperforming many competitors and being quite flexible. It is especially well suited to problems with many variables (up to thousands) with sparse constraints (that is, constraints that depend only on small subsets of variables). It is capable of handling equality and inequality constraints.

This solver allows for the specification of lower and upper bounds of variables separately to the specification of inequality constraints. Variable bounds are guaranteed to be respected at all iterations; inequality constraints are only guaranteed to be satisfied at the converged solution, if the problem is feasible. This distinction is important because some constraints define the domain of problem and should never be violated; other constraints are problem-based and therefore can be violated during the iteration process.

Finally, Ipopt is built with sparsity in mind. Complex calculations should be broken into simpler constraints, each depending on less variables. This may even increase the number of variables but Ipopt's performance profits from this structure.

## 4.5 Lambert problem implementation

The formulations stated in the previous chapter make for one-dimensional nonlinear programs, which leads to high performance. However, they do not handle the singularity case of  $\mathbf{r}_1 \parallel \mathbf{r}_2$ , which is of particular importance to orbital maneuvers as they often happen at periapsis and apoapsis. Sukhanov's formulation actually gives expressions for the initial radial and normal velocity when the input positions are collinear; the plane of the orbit should then be adequately chosen afterwards (SUKHANOV, 2010). However, this was found to be very numerically sensitive and another algorithm was used in the rest of this work. An implicit orbit propagation algorithm, as described in Section 4.1 is setup with boundary conditions

$$\mathbf{r}_{(j=1)} = \mathbf{r}_1 \quad (4.2)$$

$$\mathbf{r}_{(j=N+1)} = \mathbf{r}_2 \quad (4.3)$$

which account for the 6 boundary conditions needed. In order to help convergence in the collinear case (and neighboring cases), two inequality constraints may be added:

$$\mathbf{r}_j^T \mathbf{r}_j \geq R_{\text{Earth}}^2 \quad (4.4)$$

$$\mathbf{r}_j \times \mathbf{v}_j \geq 0 \quad (4.5)$$

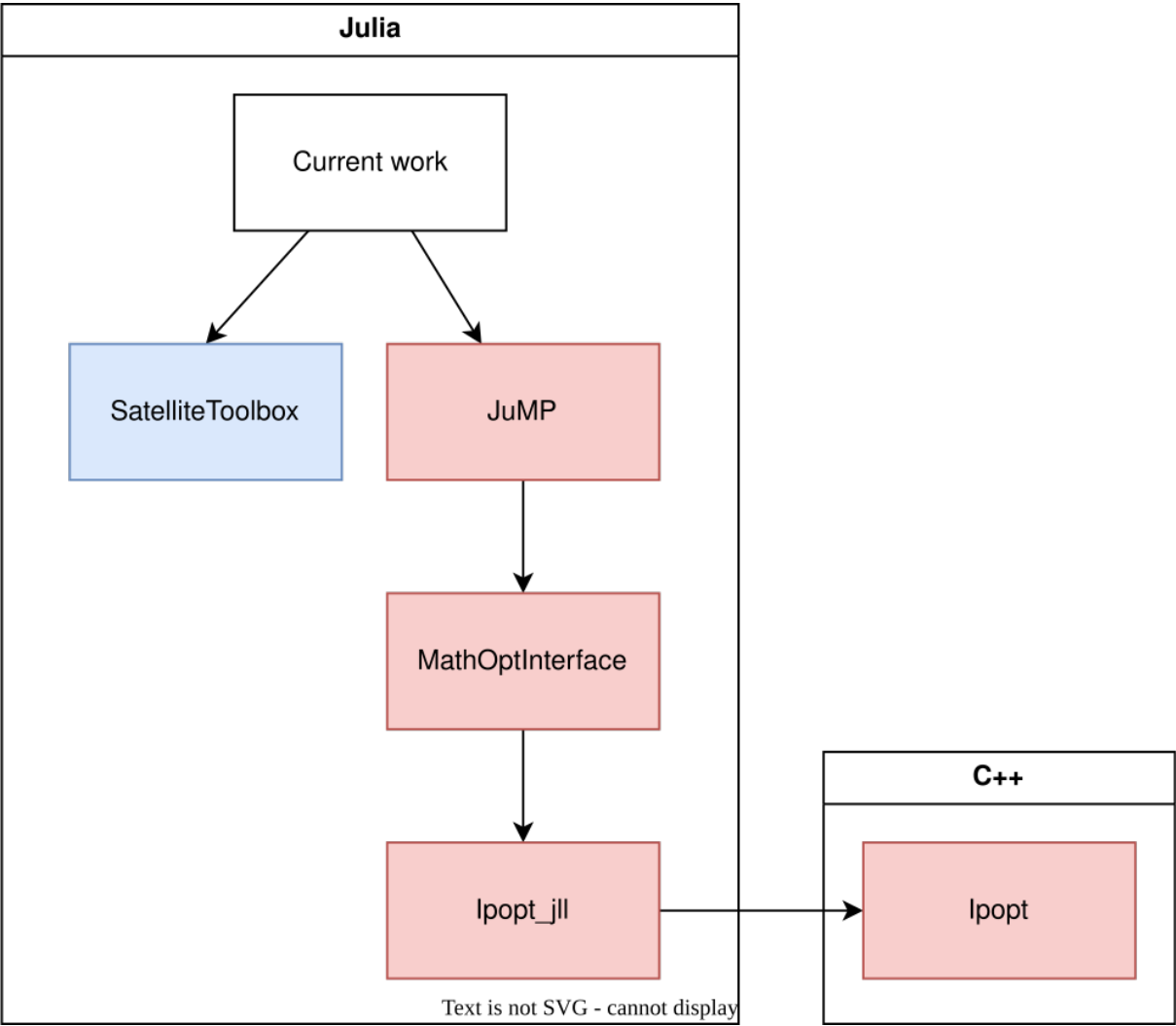


FIGURE 4.1 – Relationship of code components.

where the second constraint must be inverted if the desired orbit is retrograde.

The propagation variables are initialized with the initial position and velocity.

## 4.6 Optimal impulsive maneuver problem statement

The full optimization problem, as it is implemented in code, shall be stated in this section. Due to JuMP's intuitive modelling language, the problem is coded almost as it is stated here. The input parameters are:

1.  $\mathbf{r}_1, \mathbf{v}_1$ : initial orbital position and velocity;
2.  $\mathbf{r}_2, \mathbf{v}_2$ : final orbital position and velocity;
3.  $t_f$ : transfer time;
4.  $N$ : number of integration steps per coasting arc.

The problem comprises the following variables, where inequalities represent variable bounds:

1.  $\Delta t_1 \geq 0, \Delta t_2 \geq 0$ : intervals between 0 and the first maneuver and between the first and second maneuver;
2.  $\Delta v_1 \geq 0, \Delta v_2 \geq 0$ <sup>1</sup>: magnitudes of the first and second impulses;
3.  $\hat{\mathbf{u}}_1, \hat{\mathbf{u}}_2 \in \mathbb{R}^3$ : directions of the first and second impulses;
4.  $\chi_1, \chi_2, \chi_3 \in \mathbb{R}^{6 \times (N+1)}$ : arrays of state variables for each coasting arc. They shall be indexed as  $\chi_c^{kj}$ ,  $c = 1, 2, 3$  is the coasting arc index,  $k = 1, \dots, 6$  is the component index,  $j = 1, \dots, N + 1$  is the state vector index.  $\mathbf{x}_c^j, \mathbf{r}_c^j, \mathbf{v}_c^j$  denote the j-th state, position and velocity vectors of the c-th coasting arc:  $(\mathbf{x}_c^j)_k = \chi_c^{kj}$ .

---

<sup>1</sup>The problem could have been parameterized with vector quantities for the changes in velocities,  $\Delta \vec{v}$ , but the objective function would then be stated  $\sum \sqrt{\Delta \vec{v}^T \Delta \vec{v}}$ , which is not differentiable at  $\Delta \vec{v} = 0$ , which is inconvenient.

These variables are then subjected to constraints:

$$\text{Total time less than transfer time} \quad \Delta t_1 + \Delta t_2 \leq t_f \quad (4.6)$$

$$\text{Unit directions} \quad \Delta \hat{\mathbf{u}}_m^T \Delta \hat{\mathbf{u}}_m = 1, m = 1, 2 \quad (4.7)$$

$$\text{Initial state} \quad \mathbf{x}_1^1 = \begin{bmatrix} \mathbf{r}_1 \\ \mathbf{v}_1 \end{bmatrix} \quad (4.8)$$

$$\text{Final state} \quad \mathbf{x}_3^{N+1} = \begin{bmatrix} \mathbf{r}_2 \\ \mathbf{v}_2 \end{bmatrix} \quad (4.9)$$

$$\text{Maneuver boundary conditions} \quad \mathbf{x}_{i+1}^1 = \mathbf{x}_i^{N+1} + \begin{bmatrix} 0_{3 \times 1} \\ \Delta v_i \hat{\mathbf{u}}_i \end{bmatrix}, i = 1, 2 \quad (4.10)$$

$$\text{Propagation of coasting arcs} \quad \mathbf{x}_c^{j+1} = f_{RK}(\mathbf{x}_c^j, \Delta t_c/N), c = 1, 2, 3, j = 1, \dots, N \quad (4.11)$$

$$\text{where} \quad \Delta t_3 = t_f - \Delta t_1 - \Delta t_2 \quad (4.12)$$

$$(4.13)$$

Finally, the objective is given by

$$\min \Delta v_1 + \Delta v_2 \quad (4.14)$$

The solver should be initialized with a feasible, but not necessarily optimal solution, for better convergence (since Ipopt is a local solver, the choice of initial guesses is important). Values for  $\Delta t_1$  and  $\Delta t_2$  should be proposed based on physical reasoning. Then, the variables of the first and last coasting arcs are initialized with direct orbital propagation results (computed with the **SatelliteToolbox** package). The second coasting arc, between the impulses, is initialized with the solution to the Lambert problem between the final position of the first coasting arc and the initial position of the last coasting arc. Finally, the variables concerning the impulses' magnitudes and directions are initialized with the difference in velocity between consecutive arcs.

# 5 Results

## 5.1 Two Body

### 5.1.1 Circle to Circle

Element	Initial	Final
$a$	7000.0 km	9000.0 km
$e$	0.0	0.0
$i$	51.0°	51.0°
$\Omega$	0.0°	0.0°
$\omega$	0.0°	0.0°
$\theta$	0.0°	180.0°
Transfer time	3560.541	

TABLE 5.1 – Orbital elements used for the Hohmann transfer case analysis

Maneuver type		ICI	
$L$ (m)	$T$ (s)	$\varepsilon$	$\Delta x_f$ (m)
8.0e6	1.0	0.0	0.0
$\max\ p\ $	1.0	<b>Diagnostic</b>	Local optimum
<b>Impulse</b>	$t$ (s)	$\Delta v$ (m/s)	$1 - p \cdot \hat{u}$
1	0.0	457.74489	0.0
2	3560.54079	429.8171	0.0
<b>Total</b>	3560.54079	887.56199	

### 5.1.2 Noncoplanar rendez-vous

Maneuver type		ICI	
$L$ (m)	$T$ (s)	$\varepsilon$	$\Delta x_f$ (m)
6.7631e6	11107.158	1.00e-06	0.0
$\max\ p\ $	1.0	<b>Diagnostic</b>	Local optimum
<b>Impulse</b>	$t$ (s)	$\Delta v$ (m/s)	$1 - p \cdot \hat{u}$
1	0.0	11740.94035	-0.0
2	11107.1576	11708.69678	-0.0
<b>Total</b>	11107.1576	23449.63713	

Maneuver type		CICIC	
$L$ (m)	$T$ (s)	$\varepsilon$	$\Delta x_f$ (m)
6.7631e6	11107.158	1.00e-06	0.0
$\max\ p\ $	3.327	<b>Diagnostic</b>	Add impulse
<b>Impulse</b>	$t$ (s)	$\Delta v$ (m/s)	$1 - p \cdot \hat{u}$
1	6644.30733	37.29252	-0.0
2	10689.86179	16.20984	-0.0
<b>Total</b>	11107.1576	53.50237	

Maneuver type		CICICIC	
$L$ (m)	$T$ (s)	$\varepsilon$	$\Delta x_f$ (m)
6.7631e6	11107.158	1.00e-05	0.0
$\max\ p\ $	1.9638	<b>Diagnostic</b>	Add impulse
<b>Impulse</b>	$t$ (s)	$\Delta v$ (m/s)	$1 - p \cdot \hat{u}$
1	3370.1071	11.76294	-0.0
2	6774.61652	10.56494	0.0
3	9176.42663	20.74554	-0.0
<b>Total</b>	11107.1576	43.07342	

Maneuver type		CICICICIC	
$L$ (m)	$T$ (s)	$\varepsilon$	$\Delta x_f$ (m)
6.7631e6	11107.158	1.00e-05	0.04983
$\max\ p\ $	1.0046	<b>Diagnostic</b>	Add impulse
<b>Impulse</b>	$t$ (s)	$\Delta v$ (m/s)	$1 - p \cdot \hat{u}$
1	0.00394	3.58823	0.0
2	6724.60052	9.34687	-0.0
3	9217.50949	15.01486	-0.0
4	11107.15747	8.19599	-0.0
<b>Total</b>	11107.1576	36.14596	

## 5.2 J2 Perturbed

### 5.2.1 Circle to Circle

Maneuver type		ICI	
$L$ (m)	$T$ (s)	$\varepsilon$	$\Delta x_f$ (m)
8.0e6	1.0	1.00e-05	0.49713
$\max\ p\ $	563.46	<b>Diagnostic</b>	Initial + Final coast
<b>Impulse</b>	$t$ (s)	$\Delta v$ (m/s)	$1 - p \cdot \hat{u}$
1	0.0	5209.47789	-0.0
2	3560.54079	4318.71793	-0.0
<b>Total</b>	3560.54079	9528.19582	

### 5.2.2 Noncoplanar rendez-vous



Maneuver type		CICIC	
$L$ (m)	$T$ (s)	$\varepsilon$	$\Delta x_f$ (m)
8.0e6	1.0	1.00e-05	4.0e-5
$\max\ p\ $	2.0864	<b>Diagnostic</b>	Add impulse
<b>Impulse</b>	$t$ (s)	$\Delta v$ (m/s)	$1 - p \cdot \hat{u}$
1	72.53153	473.46697	-0.0
2	3448.63865	438.46605	-0.0
<b>Total</b>	3560.54079	911.93302	

Maneuver type		CICICIC	
$L$ (m)	$T$ (s)	$\varepsilon$	$\Delta x_f$ (m)
8.0e6	1.0	1.00e-05	0.02201
$\max\ p\ $	1.0	<b>Diagnostic</b>	Local optimum
<b>Impulse</b>	$t$ (s)	$\Delta v$ (m/s)	$1 - p \cdot \hat{u}$
1	0.38763	451.26267	-0.0
2	1697.05494	25.16996	-0.0
3	3559.91404	416.62074	-0.0
<b>Total</b>	3560.54079	893.05336	

Maneuver type		ICI	
$L$ (m)	$T$ (s)	$\varepsilon$	$\Delta x_f$ (m)
6.7631e6	11107.158	1.00e-05	3.63678
$\max\ p\ $	65.441	<b>Diagnostic</b>	Add impulse
<b>Impulse</b>	$t$ (s)	$\Delta v$ (m/s)	$1 - p \cdot \hat{u}$
1	0.0	743.66668	-0.0
2	11107.1576	727.80415	-0.0
<b>Total</b>	11107.1576	1471.47082	

Maneuver type		CICIC	
$L$ (m)	$T$ (s)	$\varepsilon$	$\Delta x_f$ (m)
6.7631e6	11107.158	1.00e-05	0.0
$\max\ p\ $	3.8353	<b>Diagnostic</b>	Add impulse
<b>Impulse</b>	$t$ (s)	$\Delta v$ (m/s)	$1 - p \cdot \hat{u}$
1	7080.30484	24.12503	-0.0
2	10011.10872	34.14936	0.0
<b>Total</b>	11107.1576	58.27439	

Maneuver type		CICICIC	
$L$ (m)	$T$ (s)	$\varepsilon$	$\Delta x_f$ (m)
6.7631e6	11107.158	1.00e-05	0.0
$\max\ p\ $	1.0	<b>Diagnostic</b>	Final coast
Impulse	$t$ (s)	$\Delta v$ (m/s)	$1 - p \cdot \hat{u}$
1	1676.61473	5.84342	-0.0
2	7185.69293	20.83452	-0.0
3	9942.01138	29.32859	-0.0
<b>Total</b>	11107.1576	56.00653	

5.3 J2 and Drag

5.3.1 Circle to Circle

STM =

$$\begin{bmatrix} 0.0 & 0.0 & 0.0 & 0.0 \\ 0.0 & 0.0 & 0.0 & 0.0 \\ 0.0 & 0.0 & 0.0 & 0.0 \\ 2.330467902138264e-6 & 0.0 & 0.0 & -5.5673128560e-6 \\ 3.461582630528354e-13 & -1.1636671818027878e-6 & 0.0 & 0.0 \\ 4.2746985475505877e-13 & 0.0 & -1.1668007203354768e-6 & 0.0 \end{bmatrix} \tag{5.1}$$

PVDOT MATRIX =

$$\begin{bmatrix} 0.0 & 0.0 & 0.0 & 1.0 \\ 0.0 & 0.0 & 0.0 & 0.0 \\ 0.0 & 0.0 & 0.0 & 0.0 \\ 2.330467902138264e-6 & 3.461582630528354e-13 & 4.2746985475505877e-13 & 5.5673128560e-6 \\ 0.0 & -1.1636671818027878e-6 & 0.0 & 0.0 \\ 0.0 & 0.0 & -1.1668007203354768e-6 & 0.0 \end{bmatrix} \tag{5.2}$$

Maneuver type			ICI
$L$ (m)	$T$ (s)	$\varepsilon$	$\Delta x_f$ (m)
8.0e6	1.0	1.00e-05	0.49712
$\max\ p\ $	563.46	<b>Diagnostic</b>	Initial + Final coast
<b>Impulse</b>	$t$ (s)	$\Delta v$ (m/s)	$1 - p \cdot \hat{u}$
1	0.0	5209.4779	-0.0
2	3560.54079	4318.71793	-0.0
<b>Total</b>	3560.54079	9528.19583	

## 6 Planning

A Gantt chart for the planned work is presented in Figure 6.1. The planning is optimistic and the most risky section is the improvement of the code, in particular the addition of multiple revolution transfers. Thus, plenty of time has been allocated to these tasks.

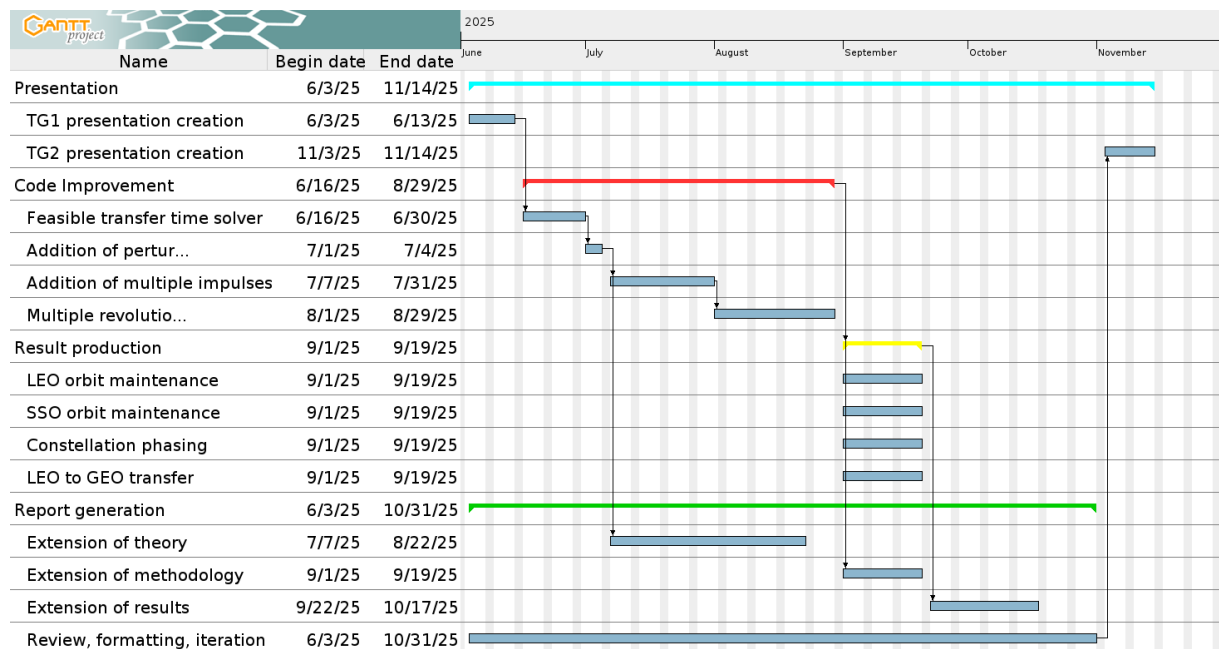


FIGURE 6.1 – Gantt Chart of planned workload.

# Bibliography

AERONAUTICS, N.; ADMINISTRATION, S. **Process for Limiting Orbital Debris**. [S.l.], 2021.

ARYA, V.; SALOGLU, K.; TAHERI, E.; JUNKINS, J. L. Generation of multiple-revolution many-impulse optimal spacecraft maneuvers. **Journal of Spacecraft and Rockets**, v. 60, n. 6, p. 1699–1711, 2023. Available at: <https://doi.org/10.2514/1.A35638>.

BATTIN, R. H.; VAUGHAN, R. M. An elegant lambert algorithm. **Journal of Guidance, Control, and Dynamics**, v. 7, n. 6, p. 662–670, 1984. Available at: <https://doi.org/10.2514/3.19910>.

BERTSEKAS, D. P. **Dynamic Programming and Optimal Control Vol. I**. 1st. ed. [S.l.]: Athena Scientific, 1995. ISBN 1886529124.

BRYSON, A. E.; HO, Y.-C. **Applied Optimal Control**. [S.l.]: Blaisdell Publishing Company, 1975.

CHAGAS, R. A. J.; CHAMBERLIN, T.; EICHHORN, H.; GAGNON, Y. L.; MENGALI, A.; BINZ, C.; SHOJI, Y.; STRA, F.; GASDIA, F.; YAMAZOE, H.; TAGBOT, J.; SRIKUMAR; CHENYONGZHI; JUSTBYOO. **JuliaSpace/SatelliteToolbox.jl: v1.0.0**. Zenodo, jan. 2025. Available at: <https://doi.org/10.5281/zenodo.14586111>.

CHOBOTOV, V. A. **Orbital Mechanics Third Edition**. [S.l.]: American Institute of Aeronautics and Astronautics, Inc., 2002.

CONWAY, B. **Spacecraft Trajectory Optimization**. [S.l.]: Cambridge University Press, 2010. (Cambridge Aerospace Series).

CURTIS, H. **Orbital Mechanics: For Engineering Students**. [S.l.]: Butterworth-Heinemann, 2020. (Aerospace Engineering).

FRANCO, T.; SANTOS, W. Gomes dos. Itasat-2: Formation flying maneuver and control considering j2 disturbances and differential drag. *In: . Proceedings [...]*. [S.l.: s.n.], 2020.

GLANDORF, D. R. Lagrange multipliers and the state transition matrix for coasting arcs. **AIAA Journal**, v. 7, n. 2, p. 363–365, 1969. Available at: <https://doi.org/10.2514/3.5109>.

JEZEWSKI, D. J.; ROZENDAAL, H. L. An efficient method for calculating optimal free-space n-impulse trajectories. **AIAA Journal**, v. 6, n. 11, p. 2160–2165, 1968. Available at: <https://doi.org/10.2514/3.4949>.

LEANDER, R.; LENHART, S.; PROTOPOPESCU, V. Optimal control of continuous systems with impulse controls. **Optimal Control Applications and Methods**, v. 36, n. 4, p. 535–549, 2015. Available at: <https://onlinelibrary-wiley-com.gorgone.univ-toulouse.fr/doi/abs/10.1002/oca.2128>.

LION, P. M.; HANDELSMAN, M. Primer vector on fixed-time impulsive trajectories. **AIAA Journal**, v. 6, n. 1, p. 127–132, 1968. Available at: <https://doi.org/10.2514/3.4452>.

LUBIN, M.; DOWSON, O.; Dias Garcia, J.; HUCHETTE, J.; LEGAT, B.; VIELMA, J. P. JuMP 1.0: Recent improvements to a modeling language for mathematical optimization. **Mathematical Programming Computation**, 2023.

LUO, Y.-Z.; ZHANG, J.; LI, H. yang; TANG, G.-J. Interactive optimization approach for optimal impulsive rendezvous using primer vector and evolutionary algorithms. **Acta Astronautica**, v. 67, n. 3, p. 396–405, 2010. ISSN 0094-5765. Available at: <https://www.sciencedirect.com/science/article/pii/S0094576510000652>.

MORELLI, A.; GIORDANO, C.; BONALLI, R.; TOPPUTO, F. Characterization of singular arcs in spacecraft trajectory optimization. 11 2023.

NASA. **ISS Environment**. 2009. Available at <https://web.archive.org/web/20080213164432/http://pdlprod3.hosc.msfc.nasa.gov/D-aboutiss/D6.html>.

OTTESEN, D.; RUSSELL, R. Unconstrained direct optimization of spacecraft trajectories using many embedded lambert problems. **Journal of Optimization Theory and Applications**, v. 191, 12 2021.

PARADISO, R. **Soyuz MS-27 Reaches the ISS in Record Time – Here’s How**. 2025. Available at <https://www.spacevoyaging.com/news/2025/04/09/soyuz-ms-27-reaches-the-iss-in-record-time-heres-how/>.

PRESS, W. H.; TEUKOLSKY, S. A.; VETTERLING, W. T.; FLANNERY, B. P. **Numerical Recipes 3rd Edition: The Art of Scientific Computing**. 3. ed. USA: Cambridge University Press, 2007. ISBN 0521880688.

PRUSSING, J. E.; CHIU, J.-H. Optimal multiple-impulse time-fixed rendezvous between circular orbits. **Journal of Guidance, Control, and Dynamics**, v. 9, n. 1, p. 17–22, 1986. Available at: <https://doi.org/10.2514/3.20060>.

SALOGLU, K.; TAHERI, E.; LANDAU, D. Existence of infinitely many optimal iso-impulse trajectories in two-body dynamics. **Journal of Guidance, Control, and Dynamics**, v. 46, n. 10, p. 1945–1962, 2023. Available at: <https://doi.org/10.2514/1.G007409>.

SCHWARZ, R. **Memorandum No. 2: Cartesian State Vectors to Keplerian Orbit Elements**. 2014. Available at <https://downloads.rene-schwarz.com/>.

SUKHANOV, A. **Lectures on Atsrodynamics**. [*S.l.*]: INPE, 2010.

TAHERI, E.; JUNKINS, J. How many impulses redux. **The Journal of the Astronautical Sciences**, v. 67, 12 2019.

Wächter, A.; Biegler, L. On the implementation of an interior-point filter line-search algorithm for large-scale nonlinear programming. **Mathematical programming**, v. 106, p. 25–57, 03 2006.

## FOLHA DE REGISTRO DO DOCUMENTO

1. CLASSIFICAÇÃO/TIPO TC	2. DATA 25 de março de 2015	3. DOCUMENTO Nº DCTA/ITA/DM-018/2015	4. Nº DE PÁGINAS 46
5. TÍTULO E SUBTÍTULO: Optimal Impulsive Orbital Maneuver Synthesis through Direct Optimization			
6. AUTOR(ES): <b>Pedro Kuntz Puglia</b>			
7. INSTITUIÇÃO(ÕES)/ÓRGÃO(S) INTERNO(S)/DIVISÃO(ÕES): Instituto Tecnológico de Aeronáutica – ITA			
8. PALAVRAS-CHAVE SUGERIDAS PELO AUTOR: Cupim; Cimento; Estruturas			
9. PALAVRAS-CHAVE RESULTANTES DE INDEXAÇÃO: Propulsão; Gás Frio; Vetorização de empuxo;			
10. APRESENTAÇÃO: <span style="float: right;">(X) Nacional   ( ) Internacional</span> ITA, São José dos Campos. Curso de Mestrado. Programa de Pós-Graduação em Engenharia Aeronáutica e Mecânica. Área de Sistemas Aeroespaciais e Mecatrônica. Orientador: Prof. Dr. Adalberto Santos Dupont. Coorientadora: Prof <sup>ra</sup> . Dr <sup>a</sup> . Doralice Serra. Defesa em 05/03/2015. Publicada em 25/03/2015.			
11. RESUMO: RESUMO			
12. GRAU DE SIGILO: <div style="display: flex; justify-content: space-around;"> <span>(X) OSTENSIVO</span> <span>( ) RESERVADO</span> <span>( ) SECRETO</span> </div>			